Cement & Concrete Composites 31 (2009) 290–300

Contents lists available at ScienceDirect

Cement & Concrete Composites

journal homepage: www.elsevier.com/locate/cemconcomp

FRP-strengthened RC beams under sustained loads and weathering

K.H. Tan [a,*], M.K. Saha [b], Y.S. Liew [c]

[a] Dept. of Civil Engineering, National University of Singapore, Blk E1A, # 07-03, 1 Engrg. Dr. 2, Singapore 117576, Singapore
[b] Structural Engineer, Global Industries Asia Pacific Pte Ltd, 41 Science Park Road, Singapore Science Park II, Singapore 117610, Singapore
[c] A/E/C Solutions Specialist, Advance Contech, 3 Raffles Place, #07-01, Singapore 048617, Singapore

ARTICLE INFO

Article history:
Received 21 December 2007
Received in revised form 17 March 2009
Accepted 20 March 2009
Available online 27 March 2009

Keywords:
Beams (support)
Cracking
Deflection
Ductility
Flexure
Fiber-reinforced polymer
Long-term serviceability
Residual strength
Sustained loads
Weathering

ABSTRACT

Glass FRP-strengthened RC beams were subjected to sustained loads and placed for different periods outdoors, indoors, and in chambers that accelerate the effects of outdoor tropical weathering by a factor of six. Beams subjected to outdoor weathering had up to 18% larger crack widths and 16% larger deflections compared to those kept indoors at the end of 1 and 2¾ years, respectively. The increase in deflections and crack widths was lesser for beams with a higher FRP reinforcement ratio. The residual flexural strength and ductility of the beams decreased with longer weathering periods. Also, the failure mode of the beams changed from concrete crushing to FRP rupture, indicating a deterioration in the mechanical properties of the FRP laminates. Analytical methods which account for material degradation in concrete and FRP laminates are presented and found to predict the long-term flexural characteristics of the beams well.

1. Introduction

Fiber-reinforced polymer (FRP) composite laminates have been popularly used in structural strengthening of reinforced concrete (RC) members due to their high strength–weight ratio and ease of installation [1,2] compared to other materials such as steel plates. However, the long-term field performance of such FRP-strengthened members has not been well established.

Limited studies have been reported on the flexural strength of FRP-strengthened RC beams subjected to weathering [3–5]. A study by Almusallam et al. [3] revealed that both solar radiation and wet–dry condition did not affect the flexural strength or rigidity of beams strengthened with glass FRP (GFRP) laminates significantly for an exposure period of 12 months. On the other hand, Leung et al. [4] reported a reduction in flexural capacity of carbon FRP-strengthened concrete beams when immersed in water for a period of 6 months. Liew [5] studied the accelerated weathering effect of tropical climate on RC beams strengthened with GFRP laminates, and concluded that a weathering period of 6–9 months resulted in the change in failure mode with a marginal drop of 2% in flexural capacity whereas weathering for more than 6 years reduced the flexural strength by 15% due to deterioration of bond between FRP laminate and concrete.

In reality, structures are subjected to sustained loading and the combined effect of sustained loading and weathering is likely to cause further degradation in the mechanical properties of concrete and FRP composite laminates. This would ultimately reduce the overall stiffness of the beam, as well as the safety margin against the ultimate collapse.

This paper reports a study on the long-term flexural characteristics of glass FRP-strengthened RC beams that were subjected to sustained loads and placed outdoors, indoors, and in weathering chambers that accelerate the effects of the outdoor tropical climate by a factor of six. Analytical methods accounting for the degradation in material properties are presented to calculate the long-term deflection and residual flexural strength of the FRP-strengthened RC beams.

2. Analytical considerations

2.1. Calculation of deflection

Under sustained loading, the concrete in the compression zone is subjected to creep which leads to a smaller effective modulus of the material and correspondingly larger beam deflections in the long-term. Similarly, the FRP laminates are subjected to tensile

* Corresponding author. Tel.: +65 65162260; fax: +65 67791635.
E-mail address: cvetankh@nus.edu.sg (K.H. Tan).

0958-9465/$ - see front matter © 2009 Elsevier Ltd. All rights reserved.
doi:10.1016/j.cemconcomp.2009.03.002

Table 1
Test program.

Beam	Total sustained load, P_s (kN)	P_s/P_1[a]	Exposure condition	Exposure duration	Remarks
(a) Small specimens (100 mm × 100 mm × 700 mm)					
A1/A2-6 m	20.4	0.53	Ambient	6 months	Beams under sustained loads in ambient laboratory condition
A1/A2-1y				1 year	
E1/E2-6 m			Exterior/outdoor	6 months	Beams under sustained loads in exterior/outdoor natural condition
E1/E2-1y				1 year	
C1/C2-5d	22.7	0.59	Chamber	5 days	Beams under sustained loads in chamber
C1/C2-15d				15 days	
C1/C2-1 m				1 month	
C1/C2-2 m				2 months	
C1/C2-3 m				3 months	
C1/C2-6 m				6 months	

Beam	ρ_{frp}[b] (%)	P_s (kN)	P_s/P_u[c]	Exposure condition	Exposure duration	Remarks
(b) Large specimens (100 mm × 125 mm × 2000 mm)						
A0-3y	0	15.8	0.59	Ambient	2¾ years	Beams under sustained loads in ambient laboratory condition
A1-3y	0.64		0.49			
A3-3y	1.92		0.40			
C1-1y	0.64	17.7	0.55	Chamber	1 year	Beams under sustained loads in chamber
C3-1y	1.92		0.45			

[a] P_1: calculated load-carrying capacity of Beam A1-0d.
[b] ρ_{frp}: FRP reinforcement ratio = FRP laminate area/cross-section area.
[c] P_u: calculated load-carrying capacity.

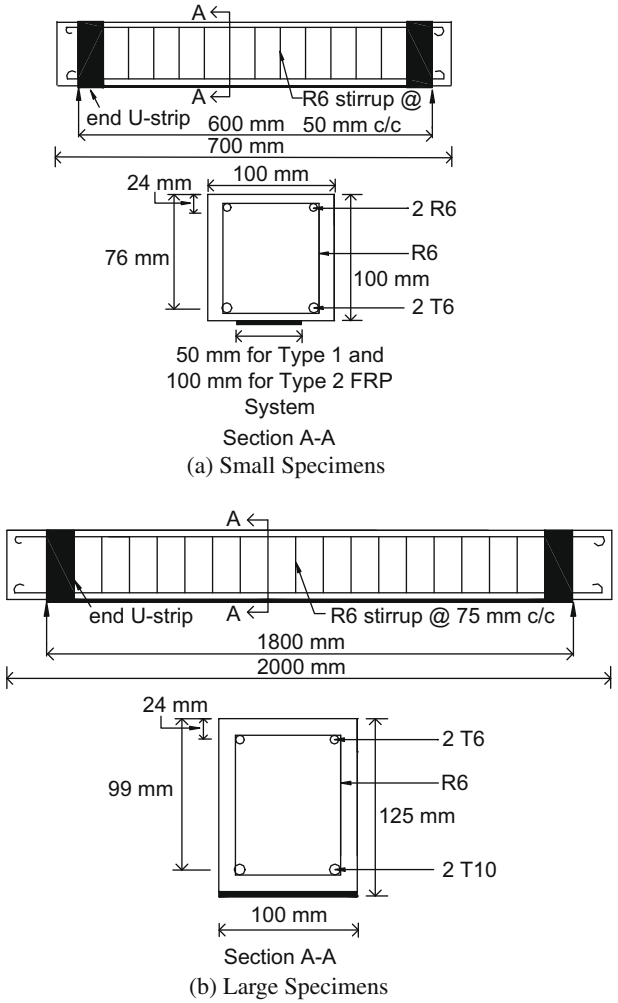

Fig. 1. Test beams and section details.

creep, leading to the same result. On the other hand, the action of weathering factors such as heat, moisture and sunlight, is to produce physiochemical processes like hydrolysis or plasticization, thermal decomposition and photo-oxidation of the polymers, causing a reduction in the modulus of the FRP laminates. However, the effect of weathering on concrete is much less significant and may therefore be neglected.

The compressive creep in concrete due to sustained loads can be accounted for by using an effective modulus of elasticity:

$$E_e = \frac{E_c}{1 + \phi_{t,t_0}} \tag{1}$$

where E_c = modulus of elasticity of concrete at age (time) t_0, t_0 = age of concrete at the time of application of loading, t = time at which deflection is to be computed, and ϕ_{t,t_0} = creep coefficient of concrete at time t as given in ACI 209R [6].

Similarly, the tensile creep of FRP laminates due to sustained loads can be accounted for using an effective modulus of elasticity, given by [7]:

$$E_{frp,t} = \frac{E_{frp}}{1 + \phi_{frp}} \tag{2}$$

where E_{frp} = initial modulus of elasticity of FRP composite laminate, and ϕ_{frp} = creep coefficient for FRP composite laminate, given by [7]:

$$\phi_{frp} = \left(\frac{t}{t_0}\right)^m - 1 \tag{3}$$

where t = time in hours after application of loading, t_0 = 1 h and m is a coefficient determined experimentally from the relation between $\varepsilon_{frp,t}$ (that is, the FRP strain at time t) and t/t_0.

To account for the effect of tropical weathering on the modulus of elasticity of FRP laminates, a residual modulus of elasticity function is defined as:

$$\varphi_{E,w} = \frac{E_{frp,w}}{E_{frp}} \tag{4}$$

where $E_{frp,w}$ = modulus of elasticity of FRP laminates at time t under the sole effect of weathering. The value of $\varphi_{E,w}$ can be established from tensile tests on weathered specimens.

The effective modulus of elasticity of FRP laminates as a result of the combined sustained loading and tropical weathering can then be taken as the product of $E_{frp,t}$ and $\varphi_{E,w}$, which in view of Eqs. (2) and (4), can be written as:

Table 2
Properties of FRP systems.

		Type 1 (unidirectional) GFRP laminate	Type 2 (bidirectional) GFRP laminate
Fiber	Type	E-Glass	E-Glass
	Sheet form	Unidirectional	Bidirectional
	Tensile strength (MPa)	1700	130
	Elastic modulus (GPa)	71	11
	Ultimate strain (%)	2.0	1.25
Resin	Type	Two part, 100% solid, low viscosity amine cured epoxy	Same as type 1 GFRP laminate
	Tensile strength (MPa)	54	
	Elastic modulus (GPa)	3	
	Ultimate strain (%)	2.5	
FRP Laminate	Volume fraction of fiber (%)	53	–
	Volume fraction of resin (%)	47	–
	Elastic modulus (GPa)	39	14[a]
	Thickness (mm)	0.8	0.7

[a] Obtained from tensile coupon tests conducted by Liew [5].

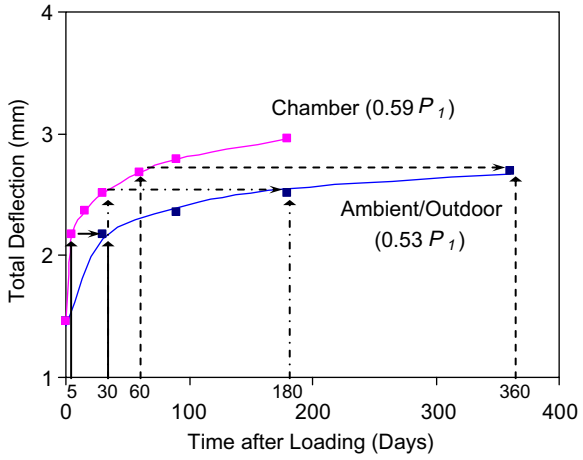

Fig. 2. Determination of equivalent sustained loads for weathering in chamber.

$$E_{frp,wt} = \varphi_{E,w} \times E_{frp,t} = \frac{\varphi_{E,w} \times E_{frp}}{1 + \phi_{frp}} = \frac{E_{frp,w}}{1 + \phi_{frp}} \tag{5}$$

With the effective modulus of elasticity of concrete and FRP laminates determined from Eqs. (1) and (5), respectively, the maximum deflection of the beam can be calculated using elastic analysis methods [7] and incorporating an effective moment of inertia based on Branson's formula [8].

2.2. Calculation of flexural strength

In this study, the sustained loads and tropical weathering are assumed to have insignificant effect on the ultimate strength and strain of concrete. The ultimate strain of FRP composite laminate after weathering under sustained loads is taken as:

$$\varepsilon_{frpu,wt} = \varphi_{\varepsilon,t} \times \varphi_{\varepsilon,w} \times \varepsilon_{frp,u} \tag{6}$$

where $\varphi_{\varepsilon,t}$ = residual ultimate strain function under sustained loading, $\varphi_{\varepsilon,w}$ = residual ultimate strain function under weathering, and $\varepsilon_{frp,u}$ = ultimate strain of virgin (that is, unweathered, non-load sustained) FRP laminate.

The value of $\varphi_{\varepsilon,t}$ is obtained as [9]:

$$\varphi_{\varepsilon,t} = \frac{\varepsilon_{frp,u} - (\varepsilon_{frp,t} - \varepsilon_{frp})}{\varepsilon_{frp,u}} = 1 - \phi_{frp}\left(\frac{\varepsilon_{frp}}{\varepsilon_{frp,u}}\right) \tag{7}$$

where ε_{frp} = instantaneous strain in FRP laminate due to sustained loads, which can be calculated from elastic bending theory using cracked section analysis, and $\varepsilon_{frp,t}$ = strain in FRP laminate at time t.

The value of $\varphi_{\varepsilon,w}$ in Eq. (6) has to be determined experimentally such as in accordance with JSCE-E-541 [10] test method. Values have been established for the GFRP systems [5] used in this study and are reported later herein.

The flexural failure modes considered were: (1) crushing of concrete in compression; (2) rupture of FRP; and (3) flexural crack induced FRP debonding. Based on the method of strain compatibility and force equilibrium, the strength corresponding to each mode of failure can be found by equating the corresponding material strain to its limiting strain.

The crushing of concrete in compression would thus occur when the strain in top compressive fiber of a section reaches the ultimate strain of concrete, that is:

$$\varepsilon_c = \varepsilon_{cu} \tag{8}$$

where ε_{cu} may be taken as 0.003. Failure by FRP rupture would happen when:

$$\varepsilon_{frp} = 0.8 \times \varepsilon_{frpu,wt} \tag{9}$$

where $\varepsilon_{frpu,wt}$ is the ultimate tensile strain of FRP laminates under combined sustained loading and tropical weathering. The coefficient of 0.8 in Eq. (9) accounts for the average lower strains of FRP rupturing when bonded to beams compared to strains measured from material tensile test [11].

Also, following Teng et al.'s [12] approach, debonding of FRP laminate from concrete strata would occur when:

$$\varepsilon_{frp} = \varepsilon_{frp,db} = \frac{1.1\beta_w\beta_l}{E_{frp,wt}}\sqrt{\frac{E_{frp,wt}\sqrt{f'_c}}{t_{frp}}} \tag{10}$$

in which, $\varepsilon_{frp,db}$ = FRP debonding strain, f'_c = concrete cylinder compressive strength, and t_{frp} = thickness of FRP laminates, β_w = bond width coefficient, and β_l = bond length coefficient.

The predicted failure mode would be the one with the lowest moment capacity.

3. Test program

Tests were carried out on two sizes of beam specimens as shown in Table 1 and Fig. 1. Two types of glass fiber-reinforced polymer (GFRP) systems, Type 1 and Type 2 as described later, were used for the smaller specimens. Type 1 GFRP system was used for strengthening of larger specimens.

The beams were designated as *Xm-t*, where '*X*' denotes the weathering condition (that is, 'A' for indoors, 'E' for outdoors and 'C' for in-chamber), '*m*' is the type of GFRP system for small specimens and the number of ply of GFRP laminate for large specimens and '*t*' indicates the actual weathering period in days (d), months (m) or years (y). For example, C1-6 m refers to a beam strengthened

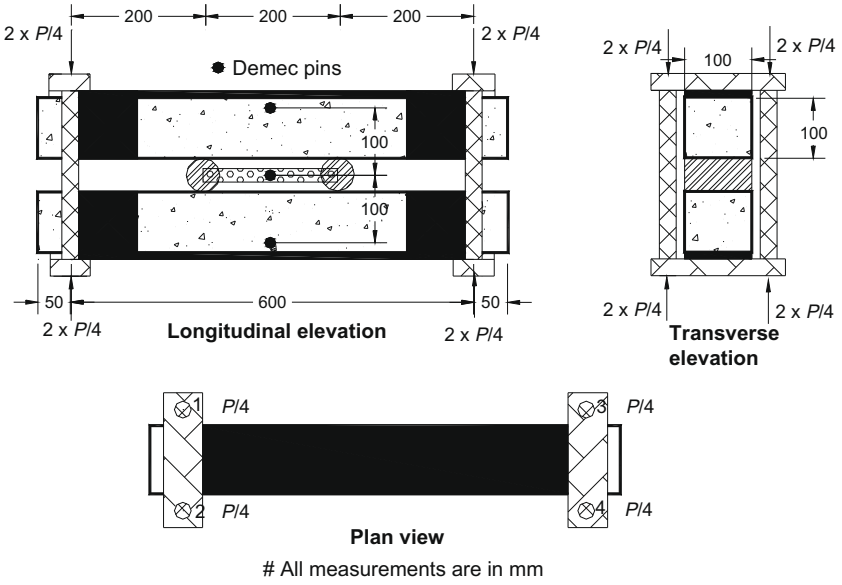

(a) Small Specimens

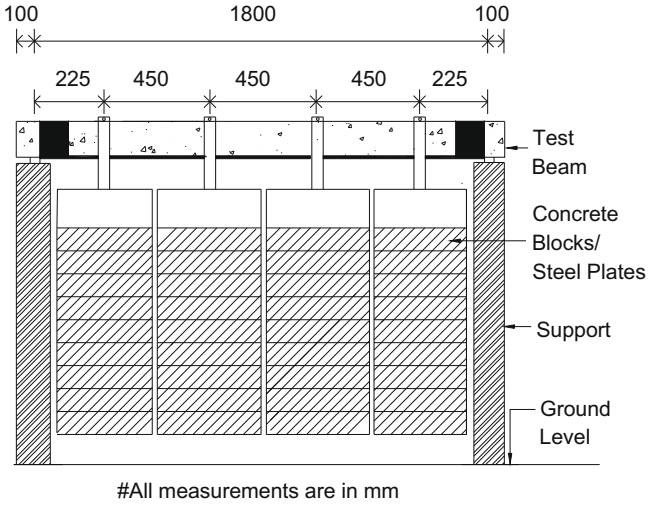

(b) Large Specimens

Fig. 3. Schematic drawing of test set-ups.

with Type 1 GFRP laminates and placed in the weathering chamber for 6 months.

3.1. Material properties

The average concrete cube compressive strength and modulus of elasticity were 42 MPa and 24.8 GPa, respectively, at 28 days. The average yield strength and modulus of elasticity of the hot-rolled deformed tensile longitudinal reinforcement averaged 525 MPa and 200 GPa, respectively.

Type 1 FRP system consisted of unidirectional roving E-glass fiber fabric that is commercially available for structural strengthening works while Type 2 FRP system consisted of bidirectional woven roving E-glass fiber fabric that is used to produce commercial products. Type 2 system has less superior mechanical properties than Type 1 system. In both systems, the fabric was impregnated with a two-part, 100% solid, and low viscosity amine cured epoxy by hand to form the laminates. The properties of glass fiber fabrics and resin, as supplied by the manufacturers, are shown in Table 2.

3.2. Installation of FRP system

For small beams, one ply of Type 1 GFRP laminate (50 mm wide and 0.8 mm thick) or Type 2 GFRP laminate, (100 mm wide and 0.7 mm thick) was installed on the tensile face of each beam. The tensile capacity of the laminates was kept the same; hence the widths of the FRP laminates were different. For large beams, Type 1 GFRP composite laminates, 100 mm in width, were applied in one ply (0.8 mm thick) for Beams A1 and C1, and in three plies (2.4 mm thick) for Beams A3 and C3. The GFRP system was installed 21 days after casting following the wet lay-out procedure. At the ends of the GFRP laminate, a carbon fiber sheet was attached transversely to prevent premature plate-end debonding during testing.

3.3. Application of sustained loads

The service load for the beams was assumed as $P_u/1.7$, where P_u is the calculated load-carrying capacity of the beam. The factor of 1.7 is based on the normal loads carried by a structural concrete member under service condition. For the small beam specimens

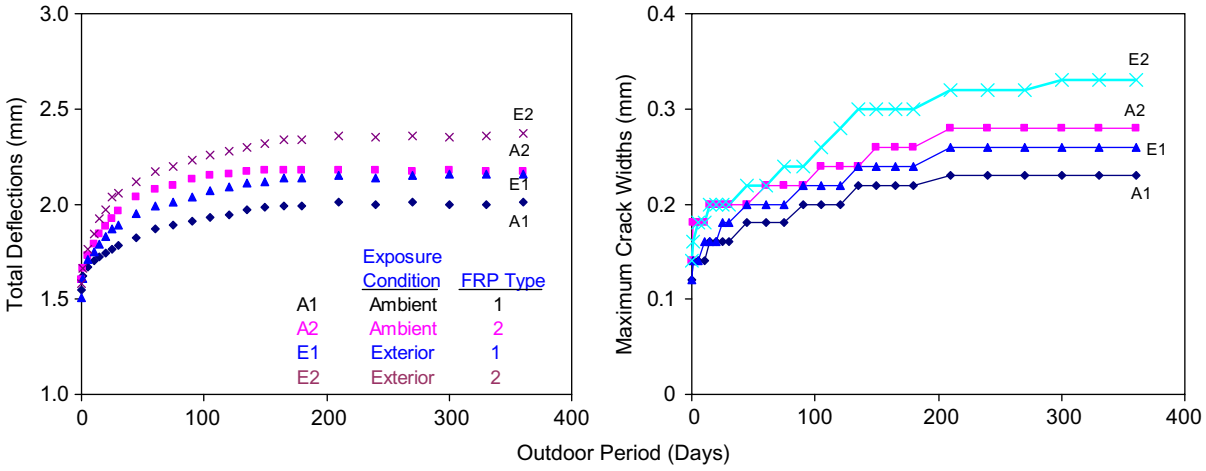

(a) Small Specimens

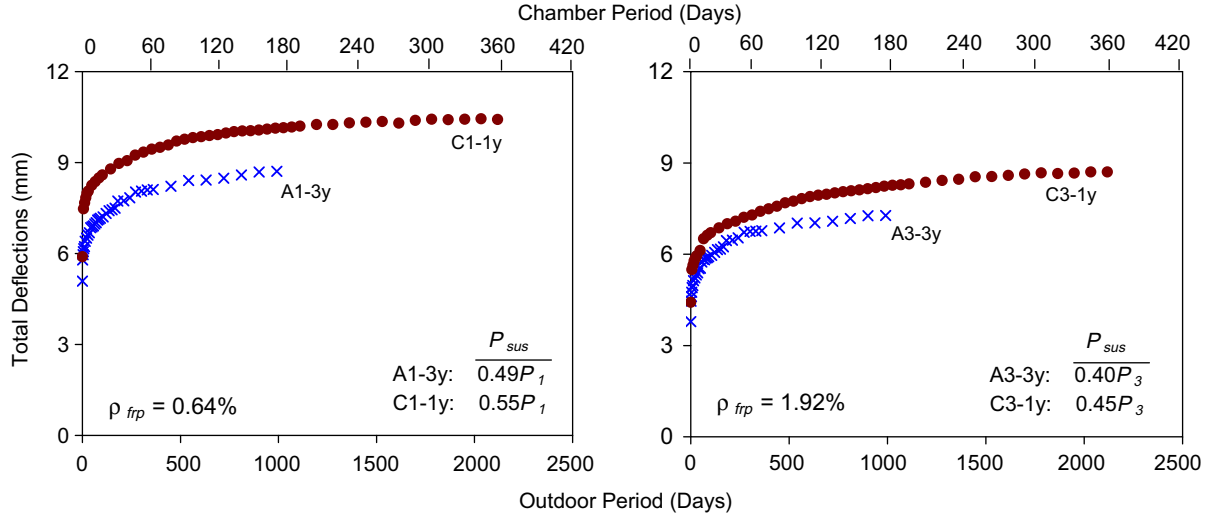

(b) Large Specimens

Fig. 4. Effect of weathering on long-term serviceability.

placed outdoors or under ambient condition, the sustained load was 90% of the service load or $0.53P_1$, where P_1 is the calculated load-carrying capacity of the beam strengthened with one ply of GFRP laminate.

For specimens placed in the weathering chamber, an equivalent sustained load had to be applied so as to accelerate the effect by a factor of six, similar to the effect of accelerated weathering (see Section 3.4). It was determined as follows. Referring to Fig. 2, first, the deflection history of the beam under a sustained load of $0.53P_1$ was computed analytically following the method explained earlier in Section 2.1 but excluding the weathering effect. Then the sustained loads to cause the same deflections at 30 days, 180 days, and 360 days in one-sixth the time were determined, and the average value was found to be equal to $0.59P_1$.

All the beams were clamped in pairs using transverse stainless steel bars at the beam ends, as shown in Fig. 3a, with steel rods placed in between the beams at one-third points, to simulate the sustained loads. The stress level was checked by continuous monitoring of strain gauges located at top concrete face, internal tensile steel bars and the FRP laminates at mid-span of the beam.

The larger beams were simply supported over a span of 1800 mm on a steel frame as shown in Fig 3b. Loads were applied using concrete blocks and steel plates at four-points along the span to simulate uniform sustained loads. The beams kept under ambient laboratory condition (A0-3y, A1-3y, and A3-3y) were subjected to a sustained load equal to the service load or 0.59 times the ultimate load-carrying capacity ($0.59P_0$) of the unstrengthened beam. This is equivalent to 0.49 times the ultimate load-carrying capacity of the beam strengthened with one ply of GFRP laminates ($0.49P_1$), or 0.40 times that of the beam strengthened with three plies of GFRP laminates ($0.40P_3$). For the two beams kept in the weathering chamber, an equivalent sustained load determined in the same manner as for small specimens equal to $0.55P_1$ was applied on C1-1y and $0.45P_3$ on Beam C3-1y.

3.4. Weathering

The tropical climate is characterized by a hot and humid weather with very little seasonal variation in temperature or precipitation throughout the year. Just north of the Equator in Singapore, the diurnal temperature rarely goes below 23 °C or above 33 °C, and the monthly rainfall ranges between 100 to 180 mm. On average, there is not less than four sunshine hours per day. Mean daily relative humidity is as high as 80–90% at night and 50–60% during the daytime.

For small beam specimens, a ferrocement weathering chamber (1500 mm × 1000 mm × 700 mm) was fabricated to simulate the outside tropical weathering effect in the laboratory [5]. By considering the outdoor average diurnal sun hour percentage and monthly rainfall fraction, a continuous light-wet-dark cycle was generated in the weathering chamber. In each cycle, the light period lasted 1.5 h, during which both the UV-A floodlight and ceramic heaters worked together to generate UV-A ray and heat that simulate the daytime weathering condition. It was then followed by 1.5 h of wet period where the entire specimens were wetted by water spraying through the atomizers, similar to outdoor wetting of specimens by the rain.

To better simulate the outdoor temperature and humidity fluctuations, 1 h of dark period (that is, idle period) was employed immediately after the light period, during which all the gadgets were switched off. Hence one cycle of weathering took 4 h and 6 cycles can be completed within a day. The natural outdoor weathering process was therefore carried out at an accelerated rate of six in the weathering chamber. This has been verified from tests on beam specimens placed outdoors and in the chamber [5].

For the large beam specimens, a weathering chamber of size 2300 mm × 1000 mm × 625 mm was constructed to enclose the beams. To reproduce all the weathering factors, the chamber was equipped with the required devices, namely UV light, ceramic heaters, thermostats, water pump and atomizers, similar to the weathering chamber for small beam specimens. The reproduction of the weathering factors at an accelerated rate of six has also been verified [13].

3.5. Instrumentation

During the weathering period, the mid-span deflection of the small beams was measured using a demec gauge system (Fig. 3) with an accuracy of 0.002 mm and the crack width was measured using a hand-held microscope which has a graduated scale in divisions of 0.02 mm. Measurements were taken upon application of sustained loads, and after 1, 3, 5, 7, 10, 14, 21 days, weekly up to 3 months, every 15 days till 6 months, and thereafter every month till the end of 1 year.

Deflections of large beams were measured using a transferable dial beam consisting of a movable frame with three dial gauges located at quarter points and mid-span. The dial gauges had an accuracy of 0.01 mm. Measurements were taken at the same time intervals as those for the small beam specimens.

At the end of the weathering period, the specimens were relieved of the sustained loads. They were then tested statically under four-point loading using the Instron universal testing machine to failure, at a constant cross-head speed of 0.2 mm/min. The mid-span deflection was monitored by a Linear Variable Displacement Transducer (LVDT). Crack widths were measured in the pure moment zone at 5 kN intervals using a hand-held microscope.

4. Test results and discussion

4.1. Long-term deflection and crack width

4.1.1. Effect of weathering

Fig. 4a compares the total deflections and crack widths of small beams under sustained loads and subjected to outdoor weathering with those kept indoors under ambient laboratory condition. The deflections of beams strengthened with Type 1 GFRP system and kept outdoors were found to be more than those kept indoors by about 7% at the end of 1 year. Similarly, for beams strengthened with Type 2 GFRP system, the difference was about 9%. On the other hand, the crack width was larger by 13% and 18%, respectively. From visual inspection, the interface between the FRP composite laminate and the concrete substrate was found to be unaffected by combined sustained loading and tropical weathering; the larger deflections and crack widths may be due to the degradation in tensile stiffness of GFRP composite laminate.

Fig. 4b shows the effect of weathering on the deflections of large beams under sustained loads. After 5½ months weathering in the chamber (equivalent to 2¾ years outdoors), Beams C1-1y (ρ_{frp} = 0.64%) and C3-1y (ρ_{frp} = 1.92%) showed about 16% and 13% larger deflections compared to Beams A1-3y (ρ_{frp} = 0.64%) and A3-3y (ρ_{frp} = 1.92%), respectively, which were kept in ambient laboratory condition. Again, the larger deflections may be due to the degradation in tensile stiffness of GFRP composite laminates due to the synergistic effect of sunlight and rainfall.

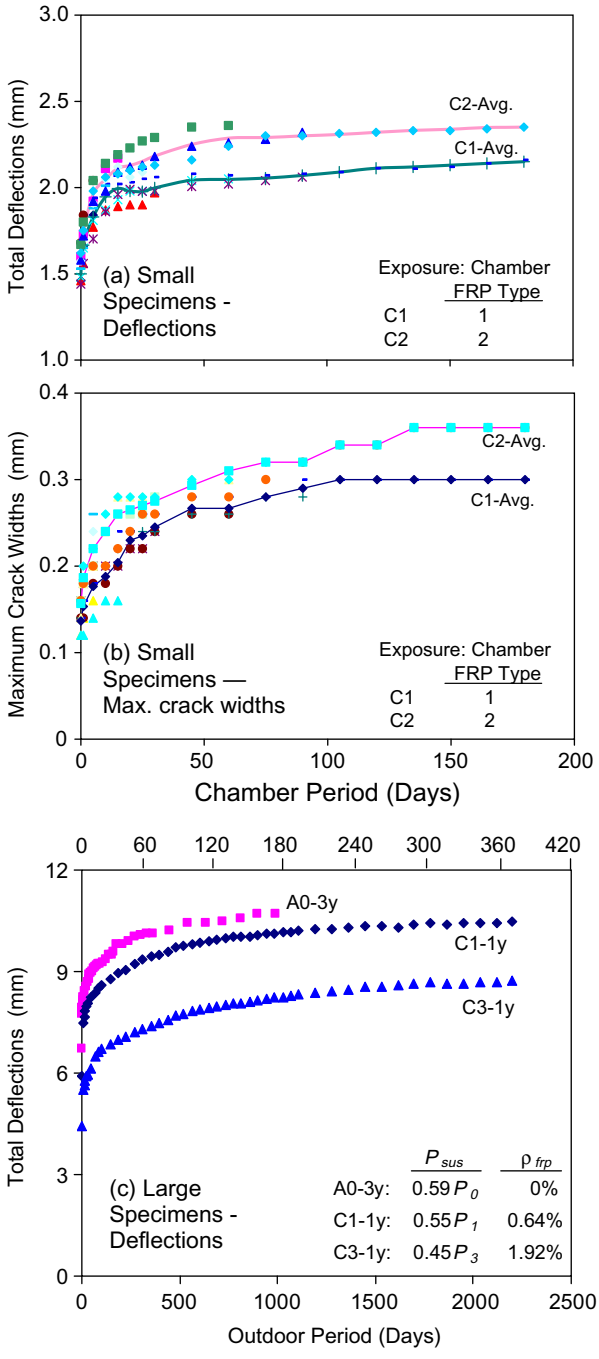

Fig. 5. Effect of FRP type and reinforcement ratio on long-term serviceability.

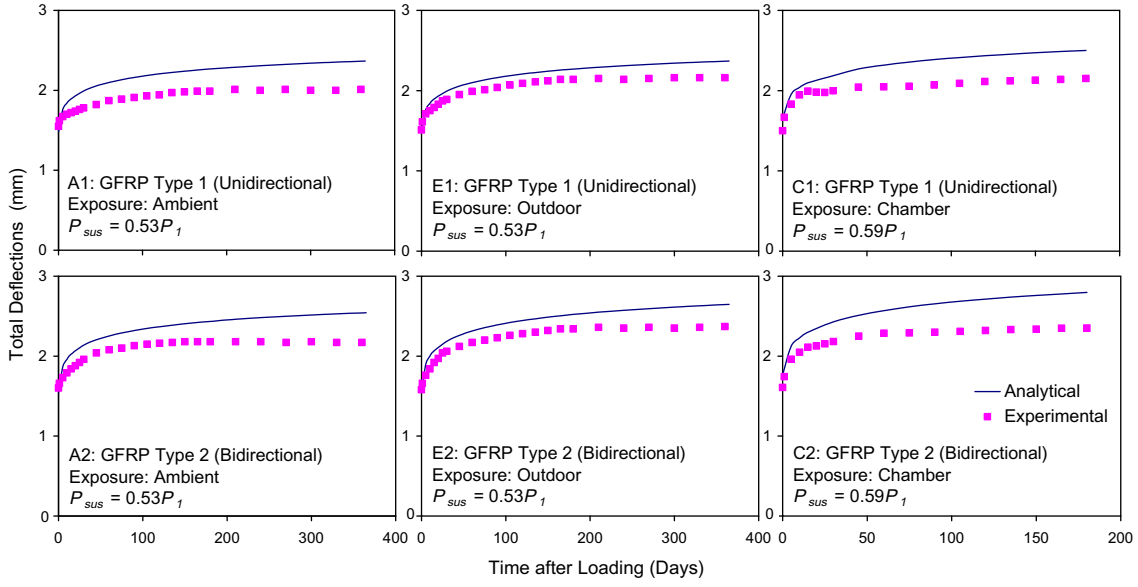

(a) Small Specimens

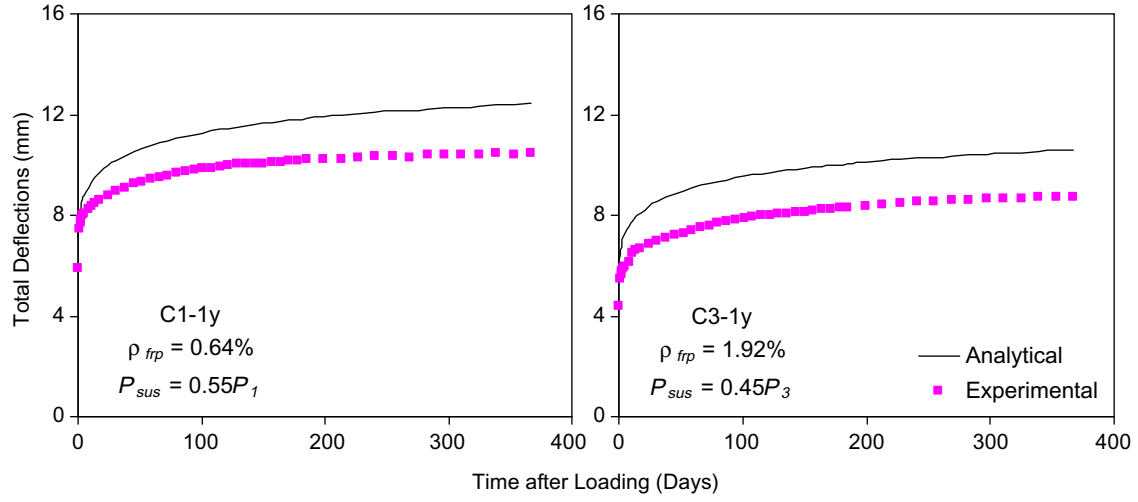

(b) Large Specimens

Fig. 6. Comparison of observed deflections with analytical predictions.

4.1.2. Effect of FRP type and reinforcement ratio

The total deflections and crack widths observed on small beams kept in the weathering chamber are shown in Fig. 5a and b, respectively. The solid lines give the average of the observed deflections and crack widths. At the end of 6 months of chamber weathering (equivalent to 3 years outdoor), beams strengthened with Type 1 FRP system showed 10% and 17% lesser deflection and crack width, respectively, compared to beams strengthened with Type 2 FRP system.

On the other hand, after 1 year outdoor weathering (Fig. 4a), beams strengthened with Type 1 GFRP system showed 9% lesser deflection compared to beams strengthened with Type 2 GFRP system. As for crack widths, it was 21% lesser (Fig. 4a). The lesser amount of fiber in the direction of stress, initial lack of straightness of the fiber, and inferior mechanical properties may be responsible for the larger deflections and crack widths observed in beams strengthened with Type 2 GFRP system.

Fig. 5c shows the effect of FRP reinforcement ratio on the deflections of the loaded beams under tropical weathering. The effect of weathering seems to be more detrimental in Beam C1 with ρ_{frp} = 0.64% than in Beam C3 with ρ_{frp} = 1.92%. Beam C1 was found to deflect 20% more than Beam C3 under the same sustained loads after 1 year of accelerated weathering. Weathering elements did not seem to result in deterioration of the interface bond within the FRP layers or between the FRP laminates and the concrete substrate in Beam C3 (ρ_{frp} = 1.92%). However, the deflections of Beams C3 and C1 were 23% and 5% lesser, respectively, compared to the control beam, A0-3y (ρ_{frp} = 0%) at the end of 5½ months in the chamber.

4.1.3. Comparison of observed deflections with analytical predictions

In the analysis, the creep coefficient of concrete established for conventional concrete of a similar strength as in the current investigation by Tan et al. [14] was used. The creep coefficient of FRP composite laminate was computed from Eq. (3) with m equal to 0.0095 for Type 1 GFRP and 0.035 for Type 2 GFRP system. These values were the average values obtained by Holmes and Just [9] from tensile creep tests on specimens subjected to stress levels (75–102 MPa for unidirectional and 36–88 MPa for bidirectional GFRP) similar to the current investigation.

Table 3
Flexural characteristics of beams after weathering.

Specimen type	Designation	P_u (kN)	w_{sl} (mm)	Δ_{sl}[a] (mm)	Δ_{yl} (mm)	Δ_{ul} (mm)	Δ_{ul}/Δ_{yl}	Failure mode	
								Obs.	Pred.
Unstrengthened small beams	A0-6 m[a]	28.44	n.a.	1.53	1.98	5.31	2.68	n.a.	n.a.
	A0-1y[a]	27.21	n.a.	1.76	2.21	6.40	2.89	n.a.	n.a.
Small beams with Type 1 GFRP	A1-0d	45.18	0.28	2.70	3.23	10.58	3.27	CC	CC
	A1-6 m	32.98[b]	0.38	2.14	2.90	5.74	1.98	DB	CC
	A1-1y	42.30	0.20	2.03	2.50	6.51	2.60	CC	CC
	E1-6m	38.44	0.18	1.49	2.11	5.12	2.43	FR	FR
	E1-1y	40.14	0.14	1.40	1.82	5.40	2.96	FR	FR
	C1-5d	42.11	0.16	2.19	3.01	10.13	3.36	CC/DB	CC
	C1-15d	42.98	0.20	1.71	2.53	8.83	3.49	CC	CC
	C1-1 m	36.07	0.28	1.79	2.19	6.68	3.05	CC	FR
	C1-2 m	33.07	0.24	1.50	2.13	5.51	2.59	CC	FR
	C1-3 m	32.71	0.24	1.64	2.67	6.42	2.40	FR	FR
	C1-6 m	37.42	0.16	1.75	2.56	5.16	2.02	FR	FR
Small beams with Type 2 GFRP	A2-0d	39.36	0.22	2.22	2.89	7.18	2.49	CC	CC
	A2-6 m	37.02	0.14	2.39	2.85	6.13	2.15	FR	FR
	A2-1y	39.13	0.16	1.99	2.46	5.48	2.23	FR	FR
	E2-6 m	37.57	0.14	1.19	2.00	4.21	2.11	FR	FR
	E2-1y	36.41	0.14	1.10	1.93	3.78	1.96	FR	FR
	C2-5d	36.96	0.20	1.54	2.35	6.76	2.88	CC/FR	CC
	C2-15d	37.30	0.20	1.54	2.47	5.64	2.28	FR/CC	CC
	C2-1 m	26.71[b]	0.12	1.47	4.19	7.32	1.75	CC	FR
	C2-2 m	29.92[b]	0.26	1.53	2.42	5.74	2.37	FR	FR
	C2-3 m	34.75	0.18	2.43	2.99	7.38	2.47	FR	FR
	C2-6 m	34.79	0.16	1.52	2.25	4.59	2.04	FR	FR
Large beams with Type 1 GFRP	A1-0d	28.10	0.10	10.11	15.24	39.12	2.57	CC	CC
	C1-1y	24.59	0.08	6.01	12.58	15.94	1.27	FR	FR
	A3-0d	38.86	0.12	11.41	16.11	28.74	1.78	DB	CC
	C3/1y	35.68	0.13	8.79	17.39	26.75	1.54	FR	CC

Note: P_u: ultimate load; w_{sl}; max. crack width at service load (i.e., $0.59P_u$).
Δ_{sl}: deflection at service load; Δ_{yl}: deflection at steel yield load; Δ_{ul}: deflection at ult. load; n.a.: not applicable; CC: concrete crushing; DB: FRP debonding; FR: FRP rupture.
[a] Beam without FRP composite laminate.
[b] Outlier.

The residual modulus of elasticity functions due to the sole effect of weathering was established by Liew [5] using tensile coupons as follows:

$$\varphi_{E,W} = 1 - k\log(t_e) \tag{11}$$

where t_e = exposure period (in days); and k = 0.00103 and 0.00282 for Type 1 GFRP system subjected to outdoor weathering and accelerated weathering in the chamber, respectively, with corresponding values of 0.0502 and 0.0609 for Type 2 GFRP system.

The calculated deflections are compared with the test results in Fig. 6. The analytical predictions are in general conservative, but reasonably accurate. The difference between the calculated and observed deflections averaged 13% for small beams at the end of a 3 year equivalent outdoor period while for large beams, the average difference was 16% at the end of a 6 year equivalent outdoor period. The analytical results for deflection overestimated those of the tests mainly because the materials did not degraded uniformly and to the extent as the individual component materials when subjected to the same weathering conditions. That is, the inside concrete of the beam and the inner face of the laminates are not as much affected by the weathering.

4.2. Flexural strength

The flexural characteristics of all specimens tested after various time periods of weathering, is shown in Table 3. Among the small beams strengthened with Type 1 GFRP system, Beam A1-6 m showed unexpectedly low strength due to the premature debonding of GFRP laminate at the mid-span which is irrational considering the sustained load level and is therefore considered as an outlier. The other beams, in general, showed a reduction in strength with longer period of weathering. After 6 months of accelerated weathering in chamber (equivalent to 3 years of outdoor weathering), the flexural strength of beams strengthened with Type 1 GFRP laminates was reduced by about 17%, that is, comparing C1-6 m with A1-0d. However, the strength is still 32% higher than the beam without FRP strengthening (A0-6 m). Beam E1-1y that was exposed to outdoor weathering for 1 year showed only 5% reduction in flexural strength compared to Beam A1-1y which was kept under ambient condition. Beams strengthened with Type 2 GFRP laminates also showed a reduction in strength with weathering periods.

The load–deflection curves of small beams with Type 1 GFRP laminates kept inside the weathering chamber are compared with the reference Beam A1-0d in Fig. 7a. The initial stiffness of all the weathered beams was slightly lesser than that of Beam A1-0d. For short periods of weathering (up to 15 days), the beams showed improved stiffness beyond the sustained load level P_s (that is, $0.59P_1$ or 22.7 kN). The improved stiffness may be due to the initial curing of concrete and FRP laminates during short periods of weathering, which vanished quickly due to deterioration of fiber-resin bond and fiber strength with longer periods of weathering. Under outdoor weathering (Fig. 7b), however, the stiffness of the beams after 1 year seems to be not much affected compared to the companion beams kept under ambient condition.

The load–deflection curves of beams with Type 2 GFRP laminates are shown in Fig. 8. The flexural strength of Beam C2-6 m reduced by about 12% after 6 months of accelerated weathering, but the flexural strength was still 22% higher than the unstrengthened Beam A0-6 m (Fig. 8a). After 1 year, Beam E2-1y showed only 7% reduction in strength compared to Beam A2-1y (Fig. 8b).

Also, Beams C2-1 m and C2-2 m showed unexpectedly a drop in strength of 32% and 24%, respectively (see Table 3). Due to the irra-

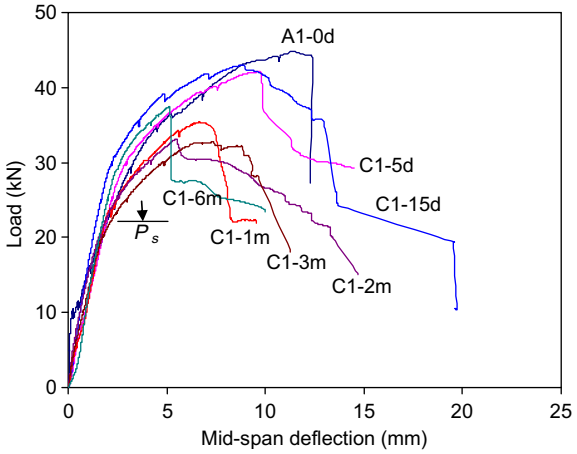

(a) Beams subjected to accelerated weathering in chamber

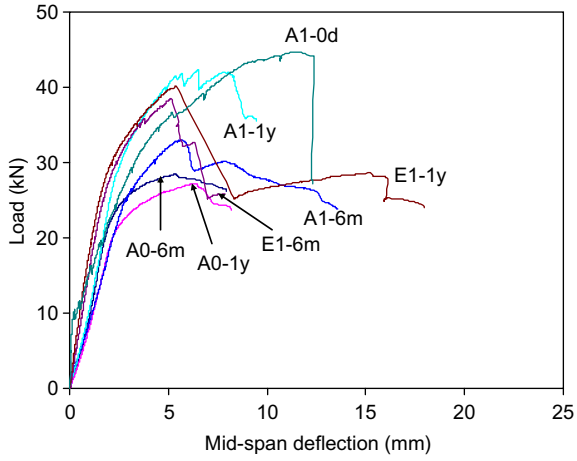

(b) Beams under ambient condition or outdoor weathering

Fig. 7. Load–deflection characteristics of small RC beams strengthened with Type 1 GFRP system.

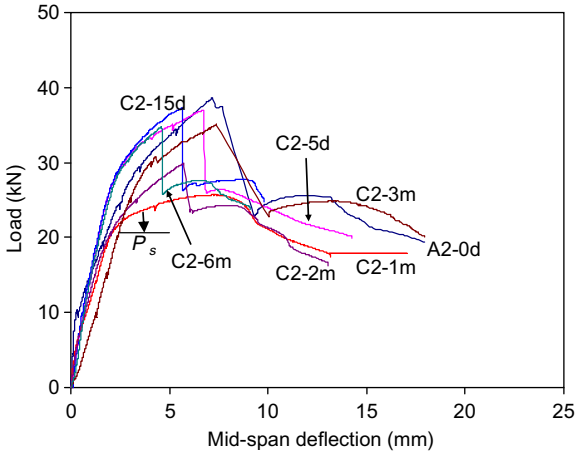

(a) Beams subjected to accelerated weathering in chamber

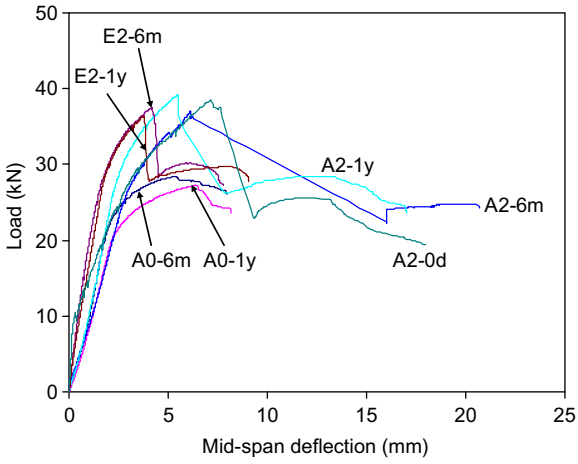

(b) Beams under ambient condition or outdoor weathering

Fig. 8. Load–deflection characteristics of small RC beams strengthened with Type 2 GFRP system.

tional low strength of Beams C2-1 m and C2-2 m, especially compared with Beams E2-6 m and E2-1y (with equivalent outdoor weathering periods) and considering the general trend, these two beams are regarded as outliers.

The flexural strength of large RC beam specimens, also reported in Table 3, is compared in Fig. 9a. For beams with ρ_{frp} = 0.64%, the reduction in flexural strength was about 13% (comparing Beam C1-1y with Beam A1-0d) whereas for beams with ρ_{frp} = 1.92%, the reduction was 8% (comparing Beam C3-1y with Beam A3-0d) at the end of 1 year of accelerated weathering (equivalent to 6 years outdoor weathering). The load–deflection curves for these beams are shown in Fig. 9b. Except for the initial permanent set, the load–deflection behavior of the weathered beams above the sustained load level remains the same as those of the virgin beams. From the results, it is evident that effect of weathering is lesser for beams with higher ρ_{frp}. This may be due to better protection against weathering elements due to thicker FRP laminates.

4.3. Ductility and failure modes

The ductility of the beams, defined as the ratio of the deflection at ultimate load (Δ_{ul}) to that at steel yield load (Δ_{yl}), was found in general to decrease with longer weathering period (see Table 3). After 6 months of accelerated weathering, the ductility of the small beams with Type 1 GFRP laminates was found to be reduced by 38%.

The ductility of RC beams strengthened with Type 2 GFRP system also seemed to decrease with longer weathering periods. For C2-6 m, the ductility reduced by 18% compared to A2-0d whereas for E2-1y, the reduction is 12% compared to Beam A2-1y.

For the large beams, the ductility was found to decrease in tandem with the strength behavior, by 50% for Beam C1-1y with ρ_{frp} = 0.64% compared to 15% for Beam C3-1y with ρ_{frp} = 1.92% at the end of 1 year accelerated weathering (Fig. 9a).

The failure mode of the beams changed from concrete crushing (CC) or flexural crack induced FRP debonding (DB) to FRP rupture (FR) with longer weathering periods. This indicates that the FRP system has deteriorated due to weathering. For beams strengthened with Type 2 GFRP system, the transition of failure mode was found to take place at an earlier age than that for beams strengthened with Type 1 GFRP system.

4.4. Comparison of test results with analytical predictions

The flexural strength of the GFRP-strengthened RC beams subjected to combined sustained loading and weathering for different time periods was calculated using the following input values. The values of $\varepsilon_{frp,u}$ for Type 1 and Type 2 GFRP laminates were taken as 0.0214 and 0.0194, respectively, as established by Liew [5]. Also, the values of $\varphi_{\varepsilon,w}$ were obtained from experimental studies [5] as:

$$\varphi_{\varepsilon,w} = a + b\log(t_e) \tag{12}$$

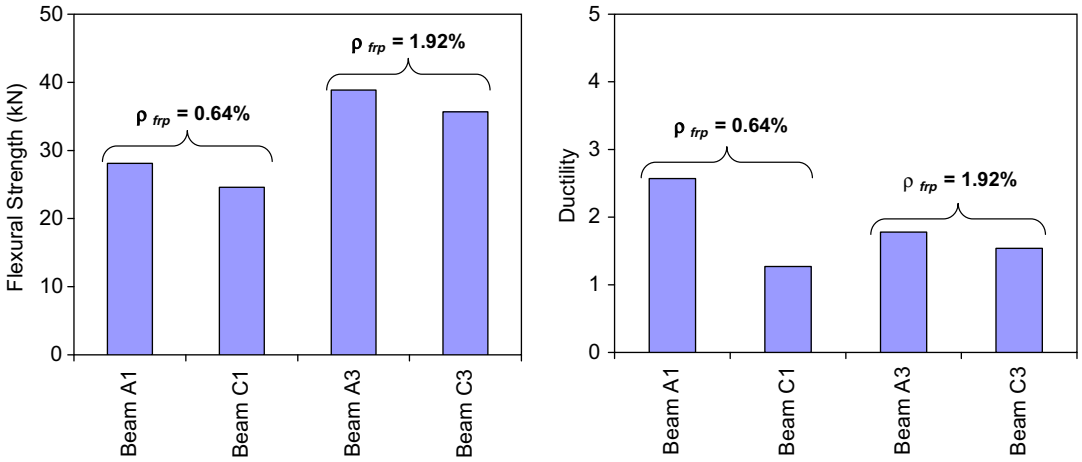

(a) Flexural strength and ductility after 6-year equivalent outdoor weathering

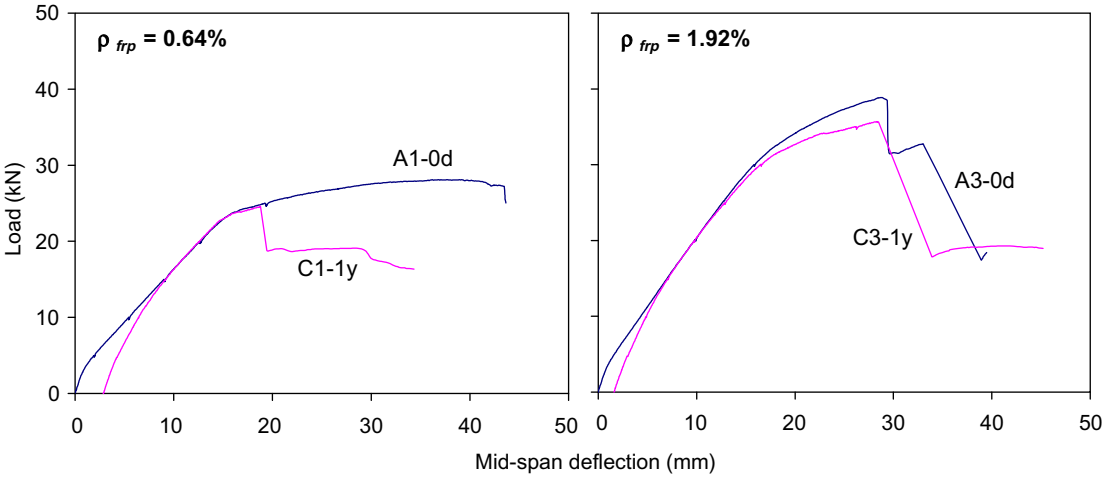

(b) Load-deflection characteristics after 6-year equivalent outdoor weathering

Fig. 9. Static behavior of large RC beams strengthened with GFRP laminates.

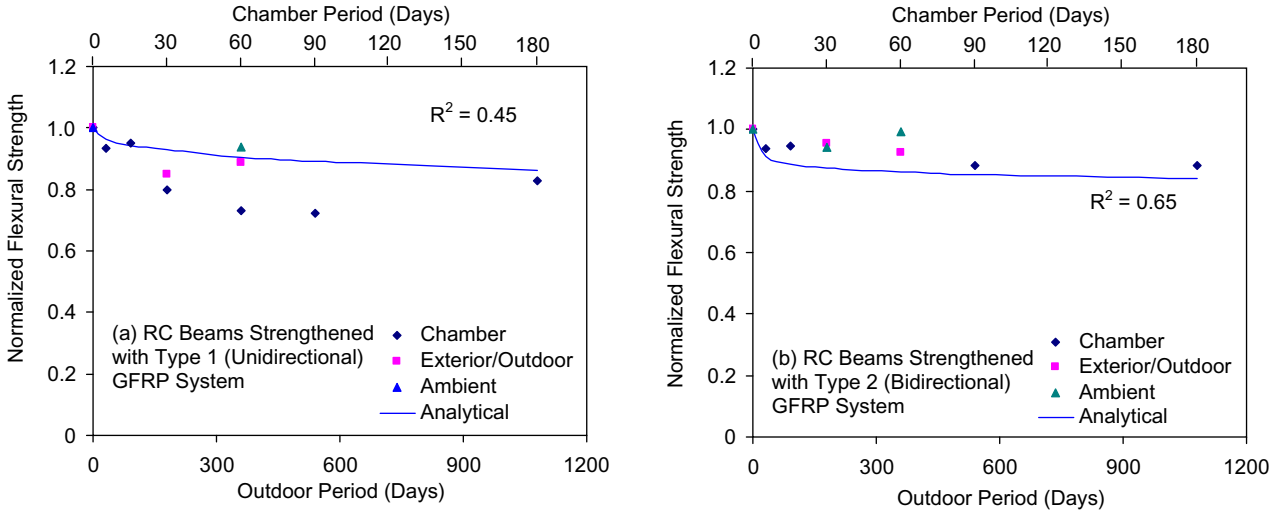

Fig. 10. Degradation in flexural strength.

where t_e = period of weathering (in days); and $(a,b) = (1.003, -0.147)$ and $(0.90, -0.151)$ for Type 1 GFRP laminates under outdoor and accelerated weathering, respectively, with corresponding values of $(0.993, -0.0133)$ and $(1.047, 0.011)$ for Type 2 GFRP laminates.

The calculated values are compared with the test results in Fig. 10. The analytical approach showed reasonable correlation with the test results except for Beams C1-2 m and C1-3 m, which are considered as outliers as explained before. Also, in general, the approach predicted the failure mode accurately as shown in Table 3.

5. Conclusions

From the analytical and experimental investigations carried out on glass FRP-strengthened RC beams under the combined effect of sustained loading and tropical weathering, the following conclusions can be drawn:

1. FRP-strengthened RC beams under sustained loads exhibited larger deflections and crack widths, when subjected to tropical weathering at the same time. They showed smaller deflections and crack widths when strengthened with a higher FRP reinforcement ratio.
2. Both the strength and ductility of beams under sustained loads decreased with the longer weathering periods. However, beams with more FRP laminates showed less degradation in strength and ductility. The failure mode changed from concrete crushing or flexural crack induced FRP debonding to FRP rupture, indicating degradation in the properties of the FRP system.
3. The proposed analytical approach, utilizing the degraded modulus of concrete and FRP laminates, gives a reasonably accurate estimate of the long-term deflection of beams subjected to sustained loading under tropical climate. The degradation in flexural strength and change in failure mode are also predicted reasonably well.

Acknowledgment

The study was supported by a research Grant R-264-000-140-112 provided by the National University of Singapore.

References

[1] ACI Committee 440. State-of-the-art report on fiber reinforced polymer (FRP) reinforcement for concrete structures (ACI440R-07). American Concrete Institute; 2007.
[2] ACI Committee 440. Guide for the design and construction of externally bonded FRP systems for strengthening concrete structures (ACI440.2R-08). American Concrete Institute; 2008.
[3] Almusallam TH, Al-Salloum YA, Alsayed SH, Mosallam AS. Durability and long-term behavior of reinforced concrete beams strengthened with FRP composites. In: Teng JG, editor. Proceedings International Conference on FRP Composites in Civil Engineering, vol. II. Hong Kong: Elsevier; 2001. p. 1579–88.
[4] Leung HY, Balendran RV, Lim CW. Flexural capacity of strengthened concrete beams exposed to different environmental conditions. In: Teng JG, editor. Proceedings International Conference on FRP Composites in Civil Engineering, vol. II. Hong Kong: Elsevier; 2001. p. 1597–606.
[5] Liew YS. Durability of FRP composites under tropical climate. MEng thesis. Singapore: National University of Singapore; 2003.
[6] ACI Committee 209. Prediction of creep, shrinkage, and temperature effects in concrete structures. Manual of concrete practice (ACI209R-92). American Concrete Institute; 1992. p. 92.
[7] Tan KH, Saha MK. Long-term deflections of RC beams externally bonded with FRP system. ASCE J Compos Constr 2006;10(6):474–82.
[8] Branson DE. Deformations of concrete structures. New York: McGraw-Hill; 1977. p. 167–9.
[9] Holmes M, Just DJ. GRP in structural engineering. Essex: Applied Science Publishers; 1983. p. 20–3 and 213–29.
[10] Japan Society of Civil Engineers. Test method for tensile properties of continuous fiber sheets (JSCE-E-541-2000). In: Japan society of civil engineers. Conc eng series, vol. 41; 2000. p. 91–105.
[11] Bonacci JF, Maalej M. Behavioral trends of RC beams strengthened with externally bonded FRP. J Compos Constr 2001;5(2):102–13.
[12] Teng JG, Chen JF, Smith ST, Lam L. FRP-strengthened RC structures. England: John Wiley & Sons Ltd.; 2002.
[13] Saha MK. Long-term behaviour of FRP-strengthened RC beams. PhD thesis. Singapore: National University of Singapore; 2007.
[14] Tan KH, Paramasivam P, Tan KC. Creep and shrinkage deflections of RC beams with steel fibers. ASCE J Mater Civil Eng 1994;6(4):394–414.